



1 **Plant functional traits modulate the effects of soil acidification on above- and**  
2 **belowground biomass**

3 Xue Feng <sup>1</sup>, Ruzhen Wang <sup>1,2</sup>, Tianpeng Li <sup>1</sup>, Jiangping Cai <sup>1</sup>, Heyong Liu <sup>1,2</sup>, Hui Li <sup>1</sup>,  
4 Yong Jiang <sup>1,2,\*</sup>

5 <sup>1</sup>Erguna Forest-Steppe Ecotone Ecosystem Research Station, Institute of Applied  
6 Ecology, Chinese Academy of Sciences, Shenyang 110016, China

7 <sup>2</sup>College of Life Sciences, Hebei University, Baoding 071002, Hebei, China

8

9 \* Correspondence: Yong Jiang ([jiangyong@iae.ac.cn](mailto:jiangyong@iae.ac.cn)).

10



11 **Abstract**

12 Atmospheric sulfur (S) deposition has been extensively recognized as a major driving  
13 force of soil acidification. However, little is known on how soil acidification influences  
14 above- and belowground biomass via altering leaf and root traits.

15 A 3-year elemental S addition were conducted to simulate soil acidification in a meadow.  
16 Grass (*Leymus chinensis*) and sedge (*Carex duriuscula*) species were chosen to  
17 demonstrate the linkage between plant traits and biomass.

18 Sulfur addition led to soil acidification and nutrient imbalance. For *L. chinensis*, soil  
19 acidification decreased specific leaf area but increased leaf dry matter content showing  
20 a conservative strategy and thus suppression of aboveground instead of belowground  
21 biomass. For *C. duriuscula*, soil acidification increased plant height and root nutrients  
22 (N, P, S, and Mn) for competing resources by investing more on above- and  
23 belowground biomass, *i.e.*, an acquisitive strategy. An overall reduction in community  
24 aboveground biomass by 3-33% was resulted from the increased soil acidity. While the  
25 community root biomass increased by 11-22% as upregulated by higher soil nutrient  
26 availability.

27 Our results provide new insights that plant above- and belowground biomass is  
28 conditioned by S-invoked acidification and their linkages with plant traits contributed  
29 to a deeper understanding of plant-soil feedback.

30 **Keywords:** sulfur addition, soil acidification, meadow grassland, functional traits,  
31 plant biomass

32



## 33 **1 Introduction**

34 Acid deposition as a consequence of anthropogenic activities will have important  
35 impacts on terrestrial biodiversity and ecosystem functions and services (Tian and Niu,  
36 2015; Clark et al., 2019; Yang et al., 2021). Atmospheric sulfur (S) deposition is one of  
37 the main causations of soil acidification, and its contribution is equal to or exceeds that  
38 of nitrogen (N) deposition in Asia (Duan et al., 2016; Zhang et al., 2022). Despite large  
39 decrease in average S deposition across China over the past decades, it is still very  
40 serious in Northeast China and Inner Mongolia (Yu et al., 2017). The northern  
41 grasslands of China as an integral part of the Eurasian grassland have experienced  
42 severe soil acidification with an overall decrease of 0.63 pH units, while S deposition  
43 can undoubtedly accelerate this process (Yang et al., 2012). Therefore, soil acidification  
44 has become a major global concern, not only leading to soil nutrient losses but also  
45 decreasing the productivity of terrestrial ecosystems (Chen et al., 2013; Tibbett et al.,  
46 2019; Duddigan et al., 2021).

47 In natural ecosystems, S limitation rarely occurred (Vitousek and Howarth, 1991;  
48 Garrison et al., 2000). Shifts in plant species and community associated with S  
49 deposition were mainly a consequence of soil acidification rather than a S-fertilization  
50 effect (Clark et al., 2019). This is because soil pH is a primary regulator of nutrient  
51 availability that plant growth and species co-existence rely on (Bolan et al., 2003;  
52 Tibbett et al., 2019). For instance, soil acidification inhibits nitrification (Kemmitt et  
53 al., 2002), but promotes the release of soil available phosphorus (P), micronutrients and  
54 the leaching of soil base cations (Jaggi et al., 2001; Chen et al., 2015; Feng et al., 2019).  
55 Evidence from contrived S addition experimentation has shown that aboveground  
56 biomass (AGB) decreased with soil acidification, whereas sedges with high acid  
57 tolerance revealed the opposite pattern in a subalpine grassland (Leifeld et al., 2011).  
58 The acidification-mediated decrease in soil cation concentrations (such as  $\text{Ca}^{2+}$  and  
59  $\text{NO}_3^-$ ) could increase the relative abundance of acid-tolerant and oligotrophic species  
60 (van Dobben and de Vries, 2010; Clark et al., 2019) as a result of decreasing abundance  
61 of other species (Jung et al., 2018). Additionally, soil Mn toxicity caused by soil



62 acidification in calcareous grassland asymmetrically curbed aboveground biomass of  
63 different species and functional groups through suppression of photosynthesis (Tian et  
64 al., 2016).

65 A global meta-analysis with most data from forest ecosystems found negative  
66 acidification effect on root biomass under sulfuric acid addition (Meng et al., 2019).  
67 This was because forest soils with low initial pH ( $\text{pH} < 5$ ) generally experienced greater  
68  $\text{Al}^{3+}$  and  $\text{Fe}^{3+}$  but less base cations, thus inhibiting root growth (Li et al., 2018).  
69 Different from findings in forests, belowground biomass increased with soil  
70 acidification in typical and alpine grasslands which was mainly due to the  
71 compensatory growth concomitant with graminoids dominating over forbs (Chen et al.,  
72 2015; Wang et al., 2020). Possibly, perennial rhizome grasses and sedges have higher  
73 ionic tolerance (such as  $\text{H}^+$ ,  $\text{Al}^{3+}$ ,  $\text{NH}_4^+$ , and  $\text{SO}_4^{2-}$ ) than perennial bunchgrasses and  
74 forbs, which allowed for the maintenance of high community biomass under soil  
75 acidification (Chen et al., 2015; Cliquet and Lemauiel-Lavenant, 2019; Wang et al.,  
76 2020). Therefore, shifts in grassland community are mainly regulated by soil nutrient  
77 fluctuations as induced by soil acidification that eventually affect above- and  
78 belowground biomass (Mitchell et al., 2018; Wang et al., 2020).

79 Functional traits substantially influence plant survival, growth and reproduction via  
80 closely associating with plant capability of resource acquisition (Violle et al., 2007).  
81 Coping with environmental stresses to persist and reproduce, plants rely on a  
82 combination of different functional traits ranging from conservative to acquisitive  
83 strategies of resource acquisition (De Battisti et al., 2020). For example, some species  
84 upregulate tissue nutrients as a fast resource acquisitive strategy when soil  
85 environmental conditions become challenging (Mueller et al., 2012). On the opposite,  
86 some plant species under environmental stresses tend to be more nutrient-conservative  
87 by developing long-lasting leaves generally with a low specific leaf area (SLA) but a  
88 high leaf dry matter content (LDMC) (Kandlikar et al., 2004). Grass species may also  
89 increase root length to avoid acid and  $\text{Al}^{3+}$  stresses (Göransson et al., 2010). In general,  
90 species with acquisitive strategy accumulate greater biomass in a rapid way, but species



91 with conservative strategy slow down biomass growth to elongate their life span (Reich,  
92 2014; Hao et al., 2020).

93 Due to difficulties in measuring grassland root traits in situ, our understanding is  
94 very limited in terms of using root trait strategy to explain the response of belowground  
95 processes to soil acidification. A pot experiment found that root length of perennial  
96 grasses decreased with soil acidification, demonstrating the constraint of root  
97 development in stressful circumstances (Haling et al., 2010). Additionally,  
98 aboveground and belowground biomass might also strongly and complicatedly be  
99 influenced by specific functional traits (Clark et al., 2019; Wang et al., 2020), soil  
100 nutrient availability, and nutrient contents and interactions in leaves and roots under  
101 soil acidification (Geng et al., 2014; Rabêlo et al., 2018; Tian et al., 2021). Overall, it  
102 still remains elusive for how soil acidification can influence the bottom-up pathway of  
103 “soil variables-functional traits-plant biomass”.

104 To understand how soil acidification influences plant traits, biomass and their  
105 relationships, we conducted a S addition experiment that included eight rates (from 0  
106 to 50 g S m<sup>-2</sup> yr<sup>-1</sup>) to simulate soil acidification in a semiarid grassland. We assessed the  
107 role of plant above- and belowground traits and soil abiotic variables in driving the  
108 grassland biomass of two dominate species (*Leymus chinensis* and *Carex duriuscula*)  
109 under soil acidification. Specifically, we also aimed to quantify how these relationships  
110 were modified by changes in soil conditions and related trait response strategy. We  
111 addressed the following questions: (i) how do soil properties (*i.e.* soil pH, Ca<sup>2+</sup>, Al<sup>3+</sup>,  
112 available N, available P), above- and belowground plant traits (*i.e.* morphological and  
113 nutrient traits) and biomass respond to different rates of S addition in the meadow  
114 grassland? (ii) What are the key traits that correlate with the biomass responses of two  
115 species to soil acidification? We hypothesize that S addition would asymmetrically  
116 affect the aboveground vs. belowground biomass in a species-specific way due to  
117 disparate trait responses of two dominate species to soil acidification (Fig. S1).

## 118 **2 Materials and methods**

### 119 **2.1 Experimental site and design**



120 This study was conducted at the Erguna Forest-Steppe Ecotone Research Station (50°  
121 10' N, 119° 23' E) of Chinese Academy of Sciences in Inner Mongolia, China. The area  
122 belongs to a transitional climate zone between mid-temperate to cold-temperate climate  
123 with mean annual temperature and precipitation of -2.45 °C and 363 mm, respectively  
124 (Feng et al., 2019). Soil in the experimental site is classified as a Haplic Chernozem  
125 according to the Food and Agricultural Organization of the United Nations  
126 classification and composed of  $37 \pm 0.9\%$  sand,  $40 \pm 1.0\%$  silt and  $24 \pm 0.8\%$  clay.  
127 Vegetation in this area is a meadow steppe community including common plant species  
128 of *Leymus chinensis*, *Stipa baicalensis*, *Cleistogenes squarrosa*, *Carex duriuscula*,  
129 *Pulsatilla turczaninovii*, and *Cymbaria dahurica*.

130 A field elemental S addition experiment was established in 2017 to simulate soil  
131 acidification caused by atmospheric S deposition. A randomized block design was  
132 exploited included eight levels of S addition (0, 1, 2, 5, 10, 15, 20, and 50 g S m<sup>-2</sup> yr<sup>-1</sup>),  
133 and each treatment had five replicates. The low dose S applications in our study was to  
134 imitate the current atmospheric SO<sub>4</sub><sup>2-</sup> deposition level (2 - 4 g S m<sup>-2</sup> yr<sup>-1</sup>) in the northeast  
135 of China (Yu et al., 2017). Each plot (6 m × 6 m) was surrounded by 2-m wide buffer  
136 strips. Purified sulfur fertilizer (elemental S > 99%) was mixed with 200 g soil collected  
137 from the untreated site nearby and applied by hand spreading annually. Sulfur powder  
138 in soil can be oxidized by soil microorganisms to form H<sup>+</sup> and SO<sub>4</sub><sup>2-</sup> which can simulate  
139 soil acidification well (Duddigan et al., 2021). In present study, we collected plant and  
140 soil samples from 25 plots (five replicates) supplemented with five levels of S (0, 5, 10,  
141 20, and 50 g S m<sup>-2</sup>yr<sup>-1</sup>).

## 142 **2.2 Plant and soil sampling**

143 On early August 2019, aboveground net primary productivity (ANPP) of plant  
144 communities was collected from peak aboveground plant biomass because all  
145 aboveground plant tissues would die during the winter. All living tissues were clipped  
146 within a randomly selected 1 m × 1 m quadrat in each plot, sorted to species and oven-  
147 dried at 65 °C for 48 h to measure peak species biomass and ANPP. The dried plant  
148 samples were prepared to measure leaf nutrients.



149 We measured three aboveground morphological traits for two dominate species  
150 *Leymus chinensis* (*L. chinensis*) and *Carex duriuscula* (*C. duriuscula*). Ten plant  
151 individuals with complete shoot were randomly selected in each plot for each species.  
152 These plant individuals were measured for maximum natural height and then clipped at  
153 the ground level. All the samples immediately placed in a portable refrigerator and then  
154 detached to measure leaf area in laboratory. To guarantee water saturation of the leaves,  
155 the sampled leaves were immersed in purified water and rehydrated for a minimum  
156 period of 6 hours. Then the water-saturated leaves were carefully wiped off the surface  
157 water with filter paper and weighed. The leaf area was scanned using a scanner (Eption  
158 Perfection V39, Seiko Epson Corporation, Japan) and then dried at 60 °C for 72 h to  
159 weigh for dry mass. Specific leaf area (SLA, cm<sup>2</sup> g<sup>-1</sup>) was calculated as the ratio of leaf  
160 area to dry mass. Leaf dry matter content was calculated as the ratio of dry mass to  
161 saturated mass (LDMC, g g<sup>-1</sup>).

162 Plant roots were sampled using the soil block method in late August 2019.  
163 Specifically, a 30 cm (length) × 30 cm (width) × 30 cm (depth) soil block was collected  
164 using a steel plate and a shovel from each plot, resulting in a total of 25 soil blocks.  
165 Each harvested soil block was immediately transported to the processing area and then  
166 the soil blocks were gently loosened by hands to separate roots from soils. All separated  
167 plant roots were carefully washed to remove the adhering soil and stored in iceboxes to  
168 the laboratory. Before determining root morphological and chemical traits, all root  
169 samples were frozen at -20 °C. At least 10 intact individual plants of *L. chinensis* and  
170 *C. duriuscula* in each plot were used for determining root nutrient traits (root [N], [P],  
171 [S], [Ca], [Fe], and [Mn]) and root morphological traits. Total root length, surface area  
172 and volume were determined using the scanned images by the software of WinRHIZO  
173 (Regent Instruments Inc., Quebec City, QC, Canada). Specific root length (SRL, m g<sup>-1</sup>)  
174 was calculated as total root length divided by its dry mass. Specific root surface area  
175 (SRA, cm<sup>2</sup> g<sup>-1</sup>) was defined as total surface area divided by its dry mass. Root tissue  
176 density (RTD, g cm<sup>-3</sup>) was obtained as the ratio of root dry mass to its volume. All of  
177 the above samples were dried at 65 °C to constant mass for determining root biomass  
178 at species and community level. Root and leaf N concentrations were determined using



179 an elemental analyzer (Vario EL III, Elementar, Hanau, Germany). Both root and leaf  
180 P, S, Ca, Fe and Mn concentrations were digested with 8 mL HNO<sub>3</sub> + 4 mL HClO<sub>4</sub> and  
181 then determined by inductively coupled plasma optical emission spectrometry (5100  
182 ICP-OES; Perkin Elmer, America).

183 Soil sampling (0 - 10 cm depth) was performed using a soil auger (5 cm inner  
184 diameter). For each plot, three cores were combined into one homogeneous sample.  
185 After removing the visible plant detritus and rock, we sieved the fresh soils through a  
186 2-mm screen and divided each soil sample into two subsamples. One subsample was  
187 immediately extracted with 2 mol L<sup>-1</sup> KCl solution. The extracted solution was analyzed  
188 for nitrate (NO<sub>3</sub><sup>-</sup>) and ammonium (NH<sub>4</sub><sup>+</sup>) concentrations using an autoAnalyser III  
189 continuous Flow Analyzer (Bran and Luebbe, Norderstedt, Germany). The other  
190 subsample was air-dried for physicochemical properties determination. Soil pH was  
191 determined in 2.5: 1 (v/w) water/soil ratio with a digital pH meter (Precision and  
192 Scientific Instrument Co. Ltd., Shanghai, China). Soil available P concentration was  
193 extracted with 0.5 mol L<sup>-1</sup> NaHCO<sub>3</sub> solution and soil available S concentration was  
194 extracted with 0.1 mol L<sup>-1</sup> Ca(H<sub>2</sub>PO<sub>4</sub>)<sub>2</sub> (Tabatabai and Bremner, 1972) following  
195 absorbance measurement on a UV-VIS spectrophotometer (UV-1700, Shimadzu, Japan)  
196 at 880 nm and 440 nm, respectively. Soil exchangeable Ca<sup>2+</sup>, Al<sup>3+</sup>, diethylene triamine  
197 pentaacetic acid (DTPA)-Fe and Mn were determined according to the methods used in  
198 our previous studies (Feng et al., 2019; Li et al., 2021).

### 199 **2.3 Statistical analyses**

200 The effects of S addition on soil properties, plant traits and biomass were analyzed using  
201 one-way analysis of variance (ANOVA) with Duncan test. Pearson's correlation  
202 analysis was used to explore the relationship between plant traits, plant biomass and  
203 soil abiotic variables across the S-addition levels. All these statistical analyses were  
204 performed using SPSS16.0 (SPSS Inc., Chicago, USA) with significance accepted at *p*  
205 < 0.05.

206 We used structural equation modelling (SEM) to analyze the direct and indirect  
207 effects of S addition meditating grassland plant aboveground and root biomass from the





208 perspective of plant traits and soil factors. Prior to SEM analysis, the number of  
209 variables were reduced by conducting principal component analysis (PCA) on soil  
210 variables (pH,  $\text{NH}_4^+\text{-N}$ ,  $\text{NO}_3^-\text{-N}$ , available P, available S, exchangeable cations  $\text{Ca}^{2+}$  and  
211  $\text{Al}^{3+}$ , DTPA-Fe and DTPA-Mn), aboveground morphological traits (Height, SLA,  
212 LDMC), leaf nutrient traits (Ca, Fe, Mn), root morphological traits (SRL, SRA, RTD)  
213 and root nutrient traits (N, P, S, Ca, Fe, Mn) of the two species (Chen et al., 2013). We  
214 then used the first principal components (PC1) for the subsequent SEM analysis to  
215 represent soil acidification (PC1 explained 94.8% of the variation), soil nutrients (PC1  
216 explained 62.3% of the variation), root nutrient traits in *C. duriuscula* (PC1 explained  
217 45.7% of the variation), aboveground morphological traits in *L. chinensis* (PC1  
218 explained 54.7% of the variation) (Table S1). A conceptual model of hypothetical  
219 relationships was constructed (Fig. S1), assuming that S addition would directly impact  
220 aboveground and belowground traits and biomass, or indirectly through altering soil  
221 pH, soil nutrient availability, soil cations and plant traits. The SEM analyses were  
222 performed using IBM SPSS AMOS 24.0 and the PCA analyses were performed using  
223 the vegan package in R 4.2.2.

224

### 225 **3 Results**

#### 226 **3.1 Effects of S addition on soil properties**

227 Sulfur addition significantly decreased soil pH from 6.95 to 5.19, but increased soil  
228 exchangeable Al concentration only in the highest S-addition level of  $50 \text{ g S m}^{-2} \text{ yr}^{-1}$   
229 (Table 1). Similarly, S addition increased soil ammonium concentration but decreased  
230 nitrate concentration in the highest S addition treatment compared to the control (Table  
231 1). Soil available P, available S, DTPA-Fe and DTPA-Mn concentration increased with  
232 increasing S addition rate, while soil exchangeable Ca concentration decreased (Table  
233 1).

#### 234 **3.2 Effects of S addition on above- and belowground traits of *L.*** 235 ***chinensis* and *C. duriuscula***



236 For the morphological traits, S addition enhanced plant height of *C. duriuscula*, but had  
237 no impact on *L. chinensis* (Fig. 1a). Sulfur addition significantly decreased SLA and  
238 increased LDMC of *L. chinensis*, whereas it had no effect on that of *C. duriuscula* (Fig.  
239 1b and c). For the belowground tissues, S treatment increased SRL in two species, and  
240 only decreased SRA of *C. duriuscula* (Fig. 1d and e). However, RTD showed no  
241 significant change for the two species (Fig. 1f).

242 For the nutrient traits, S addition had no impact on leaf [N], [P], and [Ca], and  
243 increased leaf [S] and [Mn] of the two species, while decreased leaf [Fe] of *C.*  
244 *duriuscula* but increased leaf [Fe] of *L. chinensis* (Fig. 2). An increase in root [N], root  
245 [P], root [S] of *C. duriuscula* was found under S addition, but not for *L. chinensis* (Fig.  
246 2h, i and j). Sulfur addition decreased root [Ca] of *C. duriuscula*, but had no impact on  
247 *L. chinensis* (Fig. 2k). Root [Fe] showed similar patterns with leaf [Fe] with a decrease  
248 in *C. duriuscula* and an increase in *L. chinensis* (Fig. 2l). Root [Mn] of species were  
249 enhanced by S addition (Fig. 2m).

### 250 **3.3 Effects of S addition on above- and belowground biomass**

251 In the third year, S addition suppressed aboveground biomass of plant community (Fig.  
252 3). Aboveground biomass of the two dominant species showed contrasting responses to  
253 S addition, with an increase for *C. duriuscula* but a decrease for *L. chinensis* (Fig. 3).  
254 Moreover, S addition significantly increased belowground biomass of plant community  
255 owing to the increase in *C. duriuscula*, while it had no impact on the belowground  
256 biomass of *L. chinensis* (Fig. 3).

### 257 **3.4 Correlations and pathways of S-induced soil acidification effects** 258 **on plant traits and biomass**

259 According to correlation analysis (Figs. S2 and S3), the aboveground morphological  
260 traits, leaf and the root nutrient traits showed species-specific responses. This was  
261 mainly due to the increase in soil acidity, Al<sup>3+</sup> toxicity and nutrient imbalance (*i.e.*, the  
262 deficient or excessive of certain nutrients in the soil) induced by S addition, which fitted  
263 the structural equation modelling (SEM) well ( $\chi^2 = 51.83$ ,  $P = 0.10$ ,  $df = 40$ ,  $AIC =$   
264  $103.83$ ,  $n = 25$ ) (Fig. 4). The indirect positive effect of S addition on community



265 belowground biomass was mainly implemented through decreasing soil pH together  
266 with the imbalance of soil available nutrients, altering the leaf and root nutrient traits,  
267 and the belowground biomass and of *C. duriuscula*, which accounted for 69% of the  
268 variation in community belowground biomass (Fig. 4). The indirect negative effect of  
269 S addition on community aboveground biomass was mainly achieved through soil  
270 acidification, the aboveground morphological traits and aboveground biomass of *L.*  
271 *chinensis*, which accounted for 59% of the variation in community aboveground  
272 biomass (Fig. 4).

## 273 4. Discussion

### 274 4.1 Species-specific trait responses to S addition

275 Trait response patterns was different between *L. chinensis* and *C. duriuscula* under S  
276 addition. Specifically, nutrient traits of *L. chinensis* was less plastic, as evidenced by  
277 unchanged concentrations of N, P, S, and Ca, comparing with *C. duriuscula*. Indeed, *L.*  
278 *chinensis* was suggested to be a highly homeostatic species with greater stability in  
279 elemental composition in a temperate steppe (Yu et al., 2010). Higher macroelement  
280 homeostasis helps plant maintain function and productivity stability to resist changes  
281 in soil environment (Yu et al., 2010; Feng et al., 2019).

282 It was interesting to note that both leaf and root [Fe] in *L. chinensis* increased with  
283 S addition and were not associated with soil available [Fe] (Figs. 2 and S2). Iron uptake  
284 and assimilation had been shown to be dependent on sulfate availability (Zuchi et al.,  
285 2012). Previous research demonstrated close relationships between Fe and S nutrition,  
286 suggesting common regulatory mechanisms for the homeostasis of the two elements  
287 (Fiori et al., 2013). For grasses, S addition could enhance assimilation of plant S and  
288 subsequently incorporated into methionine in order to accelerate the secretion of  
289 phytosiderophore (Zuchi et al., 2012; Courbet et al., 2019). However, Fe absorption of  
290 *C. duriuscula* was inhibited by soil acidification which was consistent with Fe (III)-  
291 reduction-based mechanism (Tian et al., 2016). Namely, acquisition of Fe by non-  
292 graminaceous monocotyledonous species was mediated by the reduction of  $\text{Fe}^{3+}$  to  $\text{Fe}^{2+}$   
293 catalyzed by the ferric chelate reductase in root cells, and  $\text{Fe}^{2+}$  absorption can be further



294 curbed by the competition with  $Mn^{2+}$  for the same metal transporter (Curie and Briat,  
295 2003; Pittman, 2005). Acidification-induced higher soil DTPA-Mn concentration in the  
296 calcareous soil contributed to Mn accumulation in plant tissues of the two species (Figs.  
297 2 and 5). Sulfur addition increased tissue [Mn] greater in *C. duriuscula* than in *L.*  
298 *chinensis*.

299 *L. chinensis* decreased SLA and increased LDMC to reduce the loss of water and  
300 nutrients, which showed conservative resource-uptake strategy under soil acidification  
301 stress. The variations in SLA and LDMC of *L. chinensis* were significantly correlated  
302 with soil exchangeable Al, implying that conservative traits might also link with Al-  
303 resistant strategy of species (Poozesh et al., 2007). As soil pH decreased, soil nitrate  
304 was reduced and positively correlated with SLA but negatively with LDMC of *L.*  
305 *chinensis* (Table 1 and Fig. S2). Soil nitrification had been shown to be positively  
306 related to leaf traits (such as leaf [N] and SLA) (Laughlin et al., 2011). This suggested  
307 that the decrease of soil nitrate under soil acidification could be an important driver of  
308 plant trait variation. For *L. chinensis*, belowground traits were insensitive to S addition  
309 as compared with *C. duriuscula*. One possible explanation for this insensitivity might  
310 be that deep-rooted species were much more resistant to changing soil environment  
311 than the shallow-rooted species (such as sedge *C. duriuscula*) (Zhang et al., 2019). We  
312 found both species invested more in enhancing SRL under soil acidification, which was  
313 in agreement with Göransson et al. (2011) that grass species increased root length to  
314 avoid acid stress. These results indicated that variation of root morphological traits has  
315 the potential to mitigate the negative effects of soil acidity and should be considered as  
316 part of stress-avoidance or tolerance strategies (Thomaes et al., 2013).

#### 317 **4.2 Species-specific and community biomass responses to S addition**

318 To clarify the underlying mechanisms, we explored the important role of morphological  
319 and nutrient traits in mediating aboveground and belowground biomass changes under  
320 S addition. We found that aboveground and root traits of two species exhibited  
321 contrasting adaptive strategies in acquiring aboveground and belowground resources  
322 which were associated with their biomass (Figs. 4 and 5). Importantly, SEM showed



323 that the decrease in aboveground biomass of *L. chinensis* was related to the increased  
324 soil acidification and the conservative responses in aboveground morphological traits  
325 under S addition (Fig. 4). *L. chinensis* seemed to be a nitrophilic and resource-  
326 acquisitive species under N-rich environment (Feng et al., 2019; Yang et al., 2019), but  
327 it was at a disadvantage under S-induced soil acidification. For example, we found SLA  
328 and LDMC in *L. chinensis* were positively correlated with the aboveground biomass of  
329 both *L. chinensis* and plant community (Fig. S2). Soil acidification resulted in enhanced  
330 toxic effects of proton and exchangeable Al (Roem and Berndse, 2000). From  
331 environmental stress hypothesis perspective, the species could employ different  
332 strategies to mitigate such environmental stress which associated with trait responses  
333 (Encinas-Valero et al., 2022). Usually, SLA and LDMC were prominent indicators of  
334 plant strategy with respect to productivity as related to environmental stress and  
335 disturbance regimes. Stress tolerant species normally had lower growth rates,  
336 photosynthetic rates, and SLA but higher LDMC (Pérez-Harguindeguy et al., 2013).  
337 Sulfur addition induced acidity stress for plants, leading to reduced SLA accompanied  
338 with lower photosynthesis and decreased plant aboveground productivity.

339 Notably, *L. chinensis* played a dominate role in aboveground productivity which  
340 was consistent with the finding that grasses occupied a mean coverage of around 60%  
341 in acid grassland and Heathland (Tibbett et al., 2019). Therefore, the decreasing  
342 aboveground biomass of *L. chinensis* was one reason for the decline of community  
343 aboveground productivity. Our results provided compelling evidences that S-induced  
344 soil acidification could alter grassland aboveground biomass via modifying shoot  
345 morphological traits mediated by soil abiotic factors. Another explanation for the  
346 decline of aboveground biomass may be competitive exclusion of bunchgrasses and  
347 forbs under soil acidification (Stevens et al., 2010; Chen et al., 2015). Our study for the  
348 first time revealed that plant leaf morphological traits might be an important regulatory  
349 factor for grassland productivity.

350 In contrast, sedge (*C. duriuscula*) was more tolerant than perennial rhizome grass  
351 (*L. chinensis*) under soil acidification. This was partly supported by similar results  
352 obtained in alpine and typical steppe grassland ecosystems (Chen et al., 2015; Wang et



353 al., 2020). Previous studies suggested that the sedge had a greater competitive  
354 advantage in nutrient-poor environments than other functional groups (Gusewell, 2004).  
355 An increase in root biomass under soil acidification suggested that sedge invested more  
356 resources in nutrient acquisition. SEM provided further evidence that for *C. duriuscula*,  
357 the higher nutrient demand (such as root [N], [P], [S], [Mn]) was matched by high root  
358 biomass investment under S treatment (Fig. 4). The increased root biomass of *C.*  
359 *duriuscula* promoted the increased belowground biomass of plant community which  
360 could be related to the shifts in soil available nutrients under S addition. Our present  
361 study provided direct evidence that *C. duriuscula* was considered to be a high nutrient-  
362 requiring species and thereby its biomass growth increased with soil acidification stress  
363 (Figs. 4 and 5). The findings suggested that the sedge played an important role in  
364 preventing grassland productivity decline in acidified soils.

365 For grassland ecosystems, most of the carbon is allocated belowground (Bontti et  
366 al., 2009). Accumulation of roots may benefit competition for nutrient and water  
367 resources in a short-term (Wang et al., 2020). In the long-term, however, asymmetric  
368 light competitive advantage of larger individuals (*L. chinensis*) rather than the  
369 competition of soil resources (DeMalach and Kadmon, 2017), will make a decisive  
370 effect on community productivity and diversity under soil acidification. Contrary to  
371 previous findings by Wang et al. (2020), who reported that diameter of 3<sup>rd</sup>-order roots  
372 contributed to the increase of community belowground biomass under soil acidification  
373 in an alpine grassland. Our study provided a novel insight that leaf and root nutrients  
374 as a whole jointly mediated community belowground biomass with soil acidification  
375 induced by S addition.

## 376 **5 Conclusion**

377 Our results highlighted that aboveground and root traits played important roles in  
378 mediating grassland plant competition for environment resources under soil  
379 acidification. Sulfur addition acidified soils, and lead to nutrient imbalance (higher  
380 ammonium, available P, Fe, Mn and exchangeable Al<sup>3+</sup>, but lower nitrate and  
381 exchangeable Ca<sup>2+</sup>). The dominate species *L. chinensis* showed conservative strategy,



382 with decreased SLA and increased LDMC in response to S addition. Moreover,  
383 conservative traits were linked with stable root biomass but lower aboveground  
384 biomass as a direct impact from soil acidification. Conversely, *C. duriuscula* displayed  
385 acquisitive strategy, with increased shoot height and root traits ([N], [P], [S], [Mn],  
386 SRL) promoting both aboveground and root biomass under S addition, as mediated via  
387 altered soil acidity and nutrient availability. Such divergent and species-specific  
388 responses was strongly driven by soil environmental conditions which resulted in  
389 inconsistent responses of grassland community aboveground and belowground biomass  
390 to S addition. As continuous S deposition causes widespread acidification and soil  
391 functional degradation problems across the world, our results implied the important  
392 roles of both aboveground and root traits in regulating species and community biomass  
393 under soil acidification.

394

395 *Author contributions.* All authors contributed to the design of the study. TL and HL  
396 conducted the experimental work and the data analysis. XF wrote the manuscript with  
397 RW, JC and YJ.

398

399 *Competing interests.* None of the authors have a conflict of interest.

400

401 *Acknowledgements.* We would like to acknowledge the support from Youth  
402 Innovation Promotion Association of Chinese Academy of Sciences.

403

404 *Financial support.* This research was supported by the National Natural Science  
405 Foundation of China (32271677, 32071563, 32222056 and 32271655), the Strategic  
406 Priority Research Program of the Chinese Academy of Sciences (XDA23080400), and  
407 the Doctoral Science Foundation of Liaoning Province (2021-BS-015).

408

409



410 *Data availability.* Data will be made available on request from the corresponding  
411 author.

412

### 413 **References**

414 Bolan, N. S., Adriano, D. C., and Curtin, D.: Soil acidification and liming interactions  
415 with nutrient and heavy metal transformation and bioavailability, *Adv. Agron.*,  
416 78, 5-272, [https://doi.org/10.1016/S0065-2113\(02\)78006-1](https://doi.org/10.1016/S0065-2113(02)78006-1), 2003.

417 Bontti, E. E., Decant, J. P., Munson, S. M., Gathany, M. A., Przeszlowska, A., Haddix,  
418 M. L., Owens, S., Burke, I. C., Parton, W. J., and Harmon, M. E.: Litter  
419 decomposition in grasslands of central North America (US Great Plains), *Global*  
420 *Chang Biol.*, 15, 1356-1363. <https://doi.org/10.1111/j.1365-2486.2008.01815.x>,  
421 2009.

422 Chen, D., Lan, Z., Bai, X., Grace, J. B., and Bai, Y.: Evidence that acidification-  
423 induced declines in plant diversity and productivity are mediated by changes in  
424 below-ground communities and soil properties in a semi-arid steppe, *J. Ecol.*,  
425 101, 1322-1334, <https://doi.org/10.1111/1365-2745.12119>, 2013.

426 Chen, D., Wang, Y., Lan, Z., Li, J., Xing, W., Hu, S. and Bai, Y.: Biotic community  
427 shifts explain the contrasting responses of microbial and root respiration to  
428 experimental soil acidification, , 90, 139-147,  
429 <https://doi.org/10.1016/j.soilbio.2015.08.009>, 2015.

430 Clark, C. M., Simkin, S. M., Allen, E. B., Bowman, W. D., Belnap, J., Brooks, M. L.,  
431 Collins, S. L., Geiser, L. H., Gilliam, F. S., Jovan, F. S., Pardo, L. H., Schulz, B.  
432 K., Stevens, C. J., Suding, K. N., Throop, H. L., and Waller, D. M.: Potential  
433 vulnerability of 348 herbaceous species to atmospheric deposition of nitrogen  
434 and sulfur in the United States, *Nat. Plants*, 5, 697-705, <https://doi.org/10.1038/s41477-019-0442-8>, 2019.

436 Cliquet, J. B. and Lemauiel-Lavenant, S.: Grassland species are more efficient in  
437 acquisition of S from the atmosphere when pedospheric S availability decreases,  
438 *Plant Soil*, 435, 69-80, <https://doi.org/10.1007/s11104-018-3872-6>, 2019.





- 439 Courbet, G., Gallardo, K., Vigani, G., Brunel-Muguet, S., Trouverie, J., Salon, C., and  
440 Ourry, A.: Disentangling the complexity and diversity of crosstalk between sulfur  
441 and other mineral nutrients in cultivated plants, *J. Exp. Bot.*, 70, 4183-4196,  
442 <https://doi.org/10.1093/jxb/erz214>, 2019.
- 443 Curie, C. and Briat, J. F.: Iron transport and signaling in plants, *Annu. Rev. Plant*  
444 *Biol.*, 54, 183-206, <https://doi.org/10.1146/annurev.arplant.54.031902.135018>,  
445 2003.
- 446 Dalle Fratte, M., Pierce, S., Zanzottera, M., and Cerabolini, B. E.: The association of  
447 leaf sulfur content with the leaf economics spectrum and plant adaptive  
448 strategies, *Plant Biol.*, 48, 924-935, <https://doi.org/10.1071/FP20396>, 2021.
- 449 De Battisti, D., Fowler, M. S., Jenkins, S. R., Skov, M. W., Bouma, T. J., Neyland, P.  
450 J., and Griffin, J. N.: Multiple trait dimensions mediate stress gradient effects on  
451 plant biomass allocation, with implications for coastal ecosystem services, *J.*  
452 *Ecol.*, 108, 1227-1240, <https://doi.org/10.1111/1365-2745.13393>, 2020.
- 453 DeMalach, N. and Kadmon, R.: Light competition explains diversity decline better  
454 than niche dimensionality, *Funct. Ecol.*, 31, 1834-1838, <https://doi.org/10.1111/1365-2435.12841>, 2017.
- 456 Duan, L., Yu, Q., Zhang, Q., Wang, Z., Pan, Y., Larssen, T., Tang, J., and Mulder, J.:  
457 Acid deposition in Asia: Emissions, deposition, and ecosystem effects,  
458 *Atmospheric Environ.*, 146, 55-69, [http://doi.org/10.1016/j.atmosenv.2016.07.](http://doi.org/10.1016/j.atmosenv.2016.07.018)  
459 018, 2016.
- 460 Duddigan, S., Fraser, T., Green, I., Diaz, A., Sizmur, T., and Tibbett, M.: Plant, soil  
461 and faunal responses to a contrived pH gradient, *Plant Soil*, 462, 505-524,  
462 <https://doi.org/10.1007/s11104-021-04879-z>, 2021.
- 463 Encinas-Valero, M., Esteban, R., Hereş, A. M., Vivas, M., Fakhret, D., Aranjuelo, I.,  
464 Solla, A., Moreno, G., and Curiel Yuste, J.: Holm oak decline is determined by  
465 shifts in fine root phenotypic plasticity in response to belowground stress, *New*  
466 *Phytol.*, 235, 2237-2251, <https://doi.org/10.1111/nph.18182>, 2022.
- 467 Feng, X., Wang, R., Yu, Q., Cao, Y., Zhang, Y., Yang, L., Dijkstra, F. A., and Jiang, Y.:  
468 Decoupling of plant and soil metal nutrients as affected by nitrogen addition in a



- 469 meadow steppe, *Plant Soil*, 443, 337-351, [https://doi.org/10.1007/s11104-019-](https://doi.org/10.1007/s11104-019-04217-4)  
470 04217-4, 2019.
- 471 Forieri, I., Wirtz, M., and Hell, R.: Toward new perspectives on the interaction of iron  
472 and sulfur metabolism in plants, *Front. Plant Sci.*, 4, 357, [https://doi.org/10.3389](https://doi.org/10.3389/fpls.2013.00357)  
473 /fpls.2013.00357, 2013.
- 474 Garrison, M. T., Moore, J. A., Shaw, T. M., and Mika, P. G.: Foliar nutrient and tree  
475 growth response of mixed-conifer stands to three fertilization treatments in  
476 northeast Oregon and north central Washington, *For. Ecol. Manag.*, 132, 183-  
477 198, [https://doi.org/10.1016/S0378-1127\(99\)00228-5](https://doi.org/10.1016/S0378-1127(99)00228-5), 2000.
- 478 Geng, Y., Wang, L., Jin, D., Liu, H., and He, J.: Alpine climate alters the relationships  
479 between leaf and root morphological traits but not chemical traits, *Oecologia*,  
480 175, 445-455, <https://doi.org/10.1007/s00442-014-2919-5>, 2014.
- 481 Göransson, P., Falkengren-Grerup, U., and Andersson, S.: *Deschampsia cespitosa* and  
482 soil acidification: general and trait-specific responses to acid and aluminium  
483 stress in a solution experiment, *Nord. J. Bot.*, 29, 97-104, [https://doi.org/10.1111](https://doi.org/10.1111/j.1756-1051.2010.00793.x)  
484 /j.1756-1051.2010.00793.x, 2011.
- 485 Gusewell, S.: N: P ratios in terrestrial plants: Variation and functional significance.  
486 *New Phytol.*, 164, 243-266, <https://doi.org/10.1111/j.1469-8137.2004.01192.x>,  
487 2004.
- 488 Hao, M., Messier, C., Geng, Y., Zhang, C., Zhao, X., and von Gadow, K.: Functional  
489 traits influence biomass and productivity through multiple mechanisms in a  
490 temperate secondary forest, *Eur. J. For. Res.*, 139, 959-968, [https://doi.org/10.](https://doi.org/10.1007/s10342-020-01298-0)  
491 1007/s10342-020-01298-0, 2020.
- 492 Haling, R. E., Richardson, A. E., Culvenor, R. A., Lambers, H., and Simpson, R. J.:  
493 Root morphology, root-hair development and rhizosheath formation on perennial  
494 grass seedlings is influenced by soil acidity, *Plant Soil*, 335, 457-468, [https://](https://doi.org/10.1007/s11104-010-0433-z)  
495 doi.org/10.1007/s11104-010-0433-z, 2010.
- 496 Jaggi, R. C., Aulakh, M. S., and Sharma, R.: Impacts of elemental S applied under  
497 various temperature and moisture regimes on pH and available P in acidic,  
498 neutral and alkaline soils, *Biol. Fert. Soils*, 41, 52-58,



- 499 <https://doi.org/10.1007/s00374-004-0792-9>, 2005.
- 500 Jung, K., Kwak, J. H., Gilliam, F. S., and Chang, S. X.: Simulated N and S deposition  
501 affected soil chemistry and understory plant communities in a boreal forest in  
502 western Canada. *J. Plant Ecol.*, 11, 511-523, <https://doi.org/10.1093/jpe/rtx030>,  
503 2018.
- 504 Kandlikar, G. S., Kleinhesselink, A. R., and Kraft, N. J.: Functional traits predict  
505 species responses to environmental variation in a California grassland annual  
506 plant community, *J. Ecol.*, 110, 833-844, [https://doi.org/10.1111/1365-](https://doi.org/10.1111/1365-2745.13845)  
507 2745.13845, 2022.
- 508 Kemmitt, S. J., Wright, D., and Jones, D. L.: Soil acidification used as a management  
509 strategy to reduce nitrate losses from agricultural land, *Soil Biol. Biochem.*, 37,  
510 867-875, <https://doi.org/10.1016/j.soilbio.2004.10.001>, 2005.
- 511 Laughlin, D.C.: Nitrification is linked to dominant leaf traits rather than functional  
512 diversity, *J. Ecol.*, 99, 1091-1099, [https://doi.org/10.1111/j.1365-2745.2011.](https://doi.org/10.1111/j.1365-2745.2011.01856.x)  
513 01856.x, 2011.
- 514 Leifeld, J., Bassin, S., Conen, F., Hajdas, I., Egli, M., and Fuhrer, J.: Control of soil  
515 pH on turnover of belowground organic matter in subalpine grassland,  
516 *Biogeochemistry*, 112, 59-69, <https://doi.org/10.1007/s10533-011-9689-5>, 2013.
- 517 Li, T., Wang, R., Cai, J., Meng, Y., Wang, Z., Feng, X., Liu, H., Turco, R. F., and  
518 Jiang, Y.: Enhanced carbon acquisition and use efficiency alleviate microbial  
519 carbon relative to nitrogen limitation under soil acidification, *Ecol. Process*, 10,  
520 1-13, <https://doi.org/10.1186/s13717-021-00309-1>, 2021.
- 521 Li, Y., Sun, J., Tian, D., Wang, J., Ha, D., Qu, Y., Jing, G., and Niu, S.: Soil acid  
522 cations induced reduction in soil respiration under nitrogen enrichment and soil  
523 acidification, *Sci. Total Environ.*, 615, 1535-1546, [http://doi.org/10.1016/j.](http://doi.org/10.1016/j.scitotenv.2017.09.131)  
524 scitotenv.2017.09.131, 2018.
- 525 Meng, C., Tian, D., Zeng, H., Li, Z., Yi, C., and Niu, S.: Global soil acidification  
526 impacts on belowground processes, *Environ. Res. Lett.*, 14, 074003, [https://](https://doi.org/10.1088/1748-9326/ab239c)  
527 doi.org/10.1088/1748-9326/ab239c, 2019.
- 528 Mitchell, R. J., Hewison, R. L., Fielding, D. A., Fisher, J. M., Gilbert, D. J.,



- 529 Hurskainen, S., Pakeman, R.J., Potts, J. M., and Riach, D.: Decline in  
530 atmospheric sulphur deposition and changes in climate are the major drivers of  
531 long-term change in grassland plant communities in Scotland, *Environ. Pollut.*,  
532 235, 956-964, <https://doi.org/10.1016/j.envpol.2017.12.086>, 2018.
- 533 Mueller, K. E., Eissenstat, D. M., Hobbie, S. E., Oleksyn, J., Jagodzinski, A. M.,  
534 Reich, P. B., Chadwick, O. A., and Chorover, J.: Tree species effects on coupled  
535 cycles of carbon, nitrogen, and acidity in mineral soils at a common garden  
536 experiment, *Biogeochemistry*, 111, 601-614, [https://doi.org/10.1007/s10533-011-](https://doi.org/10.1007/s10533-011-9695-7)  
537 9695-7, 2012.
- 538 Pérez-Harguindeguy, N., Diaz, S., Garnier, E., Lavorel, S., Poorter, H., Jaureguiberry,  
539 P., Bret-Harte, M. S., Cornwell, W. K., Craine, J. M., Gurvich, D. E., Urcelay, C.,  
540 Veneklaas, E. J., Reich, P. B., Poorter, L., Wright, I. J., Ray, P., Enrico, L.,  
541 Pausas, J. G., de Vos, A. C., Buchmann, N., Funes, G., Quetier, F., Hodgson, J.  
542 G., Thompson, K., Morgan, H. D., ter Steege, H., van der Heijden, M. G. A.,  
543 Sack, L., Blonder, B., Poschlod, P., Vaieretti, M. V., Conti, G., Staver, A. C.,  
544 Aquino, S., and Cornelissen, J. H. C.: New handbook for standardised  
545 measurement of plant functional traits worldwide, *Aust. Bot.*, 61, 167-234,  
546 <http://doi.org/10.1071/BT12225>, 2013.
- 547 Pittman, J. K.: Managing the manganese: molecular mechanisms of manganese  
548 transport and homeostasis, *New Phytol.*, 167, 733-742, [http://doi.org/10.1111/](http://doi.org/10.1111/j.1469-8137.2005.01453.x)  
549 j.1469-8137.2005.01453.x, 2005.
- 550 Poozesh, V., Cruz, P., Choler, P., and Bertoni, G., Relationship between the Al  
551 resistance of grasses and their adaptation to an infertile habitat, *Ann. Bot.*, 99,  
552 947-954, <https://doi.org/10.1093/aob/mcm046>, 2007.
- 553 Rabêlo, F. H. S., Lux, A., Rossi, M. L., Martinelli, A. P., Cuypers, A., and Lavres, J.  
554 Adequate S supply reduces the damage of high Cd exposure in roots and  
555 increases N, S and Mn uptake by Massai grass grown in hydroponics, *Environ.*  
556 *Exp. Bot.*, 148, 35-46, <https://doi.org/10.1016/j.envexpbot.2018.01.005>, 2018.
- 557 Reich, P. B.: The world-wide ‘fast-slow’ plant economics spectrum: a traits manifesto,  
558 *J. Ecol.*, 102, 275-301, <https://doi.org/10.1111/1365-2745.12211>, 2014.



- 559 Roem, W. J. and Berendse, F.: Soil acidity and nutrient supply ratio as possible factors  
560 determining changes in plant species diversity in grassland and heathland  
561 communities, *Biol. Conserv.*, 92, 151-161, <https://doi.org/10.1016/S0006-3207>  
562 (99)00049-X, 2000.
- 563 Stevens, C. J., Thompson, K., Grime, J. P., Long, C. J., and Gowing, D. J.:  
564 Contribution of acidification and eutrophication to declines in species richness of  
565 calcifuge grasslands along a gradient of atmospheric nitrogen deposition, *Funct.*  
566 *Ecol.*, 24, 478-484, <https://doi.org/10.1111/j.1365-2435.2009.01663.x>, 2010.
- 567 Thomaes, A., De Keersmaecker, L., De Schrijver, A., Baeten, L., Vandekerckhove, K.,  
568 Verstraeten, G., and Verheyen, K.: Can soil acidity and light help to explain tree  
569 species effects on forest herb layer performance in post-agricultural forests?,  
570 *Plant Soil*, 373, 183-199, <https://doi.org/10.1007/s11104-013-1786-x>, 2013.
- 571 Tian, D. and Niu, S.: A global analysis of soil acidification caused by nitrogen  
572 addition, *Environ. Res. Lett.*, 10, 024019, <https://doi.org/10.1088/1748->  
573 [9326/10/2/024019](https://doi.org/10.1088/1748-9326/10/2/024019), 2015.
- 574 Tian, Q., Liu, N., Bai, W., Li, L., Chen, J., Reich, P. B., Yu Q., Guo, D., Smith, M. D.,  
575 Knapp, A. K., Cheng, W., Lu, P., Gao, Y., Yang, A., Wang, T., Li, X., Wang, Z.,  
576 Ma, Y., and Zhang, W.: A novel soil manganese mechanism drives plant species  
577 loss with increased nitrogen deposition in a temperate steppe, *Ecology*, 97, 65-  
578 74, <https://doi.org/10.1890/15-0917.1>, 2016.
- 579 Tian, Q., Lu, P., Ma, P., Zhou, H., Yang, M., Zhai, X. Chen M., Wang, H., Li W., Bai,  
580 W., Lambers, H., and Zhang, W.: Processes at the soil-root interface determine  
581 the different responses of nutrient limitation and metal toxicity in forbs and  
582 grasses to nitrogen enrichment, *J. Ecol.*, 109, 927-938,  
583 <https://doi.org/10.1111/1365-2745.13519>, 2021.
- 584 Tibbett, M., Gil-Martinez, M., Fraser, T., Green, I. D., Duddigan, S., De Oliveira, V.  
585 H., Raulund-Rasmussen, K., Sizmur, T. and Diaz, A.: Long-term acidification of  
586 pH neutral grasslands affects soil biodiversity, fertility and function in a  
587 heathland restoration, *Catena*, 180, 401-415, <https://doi.org/10.1016/>  
588 [j.catena.2019.03.013](https://doi.org/10.1016/j.catena.2019.03.013), 2019.



- 589 van Dobben, H. and de Vries, W.: Relation between forest vegetation, atmospheric  
590 deposition and site conditions at regional and European scales, *Environ. Pollut.*,  
591 158, 921-33, <https://doi.org/10.1016/j.envpol.2009.09.015>, 2010.
- 592 Violle, C., Navas, M. L., Vile, D., Kazakou, E., Fortunel, C., Hummel, I., and Garnier,  
593 E.: Let the concept of trait be functional!, *Oikos*, 116, 882-892, [https://doi.org](https://doi.org/10.1111/j.0030-1299.2007.15559.x)  
594 [/10.1111/j.0030-1299.2007.15559.x](https://doi.org/10.1111/j.0030-1299.2007.15559.x), 2007.
- 595 Vitousek, P. M. and Howarth, R. W.: Nitrogen limitation on land and in the sea-how  
596 can it occur?, *Biogeochemistry*, 13, 87-115, <https://doi.org/10.1007/BF00002772>,  
597 1991.
- 598 Wang, P., Guo, J., Xu, X., Yan, X., Zhang, K., Qiu, Y., Zhao, Q., Huang, K., Luo, X.,  
599 Yang, F., Guo, H., and Hu, S.: Soil acidification alters root morphology,  
600 increases root biomass but reduces root decomposition in an alpine grassland,  
601 *Environ. Pollut.*, 265, 115016, <https://doi.org/10.1016/j.envpol.2020.115016>,  
602 2020.
- 603 Yang, F., Zhang, Z., Barberán, A., Yang, Y., Hu, S., Guo, H. Nitrogen-induced  
604 acidification plays a vital role driving ecosystem functions: Insights from a 6-  
605 year nitrogen enrichment experiment in a Tibetan alpine meadow, *Soil Biol.*  
606 *Biochem.*, 153, 108107, <https://doi.org/10.1016/j.soilbio.2020.108107>, 2021.
- 607 Yang, G., Lü, X., Stevens, C. J., Zhang, G., Wang, H., Wang, Z., Zhang, Z., Liu, Z.,  
608 and Han, X.: Mowing mitigates the negative impacts of N addition on plant  
609 species diversity, *Oecologia*, 189, 769-779, [https://doi.org/10.1007/s00442-019-](https://doi.org/10.1007/s00442-019-04353-9)  
610 [04353-9](https://doi.org/10.1007/s00442-019-04353-9), 2019.
- 611 Yang, Y., Ji, C., Ma, W., Wang, S., Wang, S., Han, W., Mohammat, A., Robinson, D.,  
612 and Smith, P.: Significant soil acidification across northern China's grasslands  
613 during 1980s-2000s, *Global Change Biol.*, 18, 2292-2300, [https://doi.org/10.1111](https://doi.org/10.1111/j.1365-2486.2012.02694.x)  
614 [/j.1365-2486.2012.02694.x](https://doi.org/10.1111/j.1365-2486.2012.02694.x), 2012.
- 615 Yu, H., He, N., Wang, Q., Zhu, J., Gao, Y., Zhang, Y., Jia, Y., and Yu, G.:  
616 Development of atmospheric acid deposition in China from the 1990s to the  
617 2010s, *Environ. Pollut.*, 231, 182-190,  
618 <http://doi.org/10.1016/j.envpol.2017.08.014>, 2017.



619 Yu, Q., Chen, Q., Elser, J. J., He, N., Wu, H., Zhang, G., Wu, J., Bai, Y., and Han, X.:  
620 Linking stoichiometric homeostasis with ecosystem structure, functioning and  
621 stability, *Ecol. Lett.*, 13, 1390-1399, [https://doi.org/10.1111/j.1461-0248.](https://doi.org/10.1111/j.1461-0248.2010.01532.x)  
622 2010.01532.x, 2010.

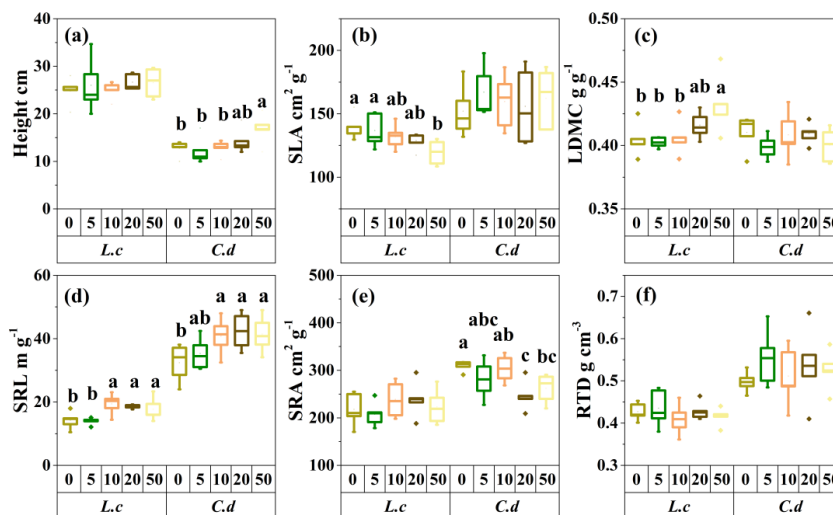
623 Zhang, B., Cadotte, M. W., Chen, S., Tan, X., You, C., Ren, T., Chen, M., Wang, S.,  
624 Li, W., Chu, C., Jiang, L., Bai, Y., Huang, J., and Han, X.: Plants alter their  
625 vertical root distribution rather than biomass allocation in response to changing  
626 precipitation, *Ecology*, 100, e02828, <https://doi.org/10.1002/ecy.2828>, 2019.

627 Zuchi, S., Cesco S., and Astolfi S.: High S supply improves Fe accumulation in  
628 durum wheat plants grown under Fe limitation, *Environ. Exp. Bot.*, 77, 25-32,  
629 <https://doi.org/10.1016/j.envexpbot.2011.11.001>, 2012.

630  
631



632 **Figures**

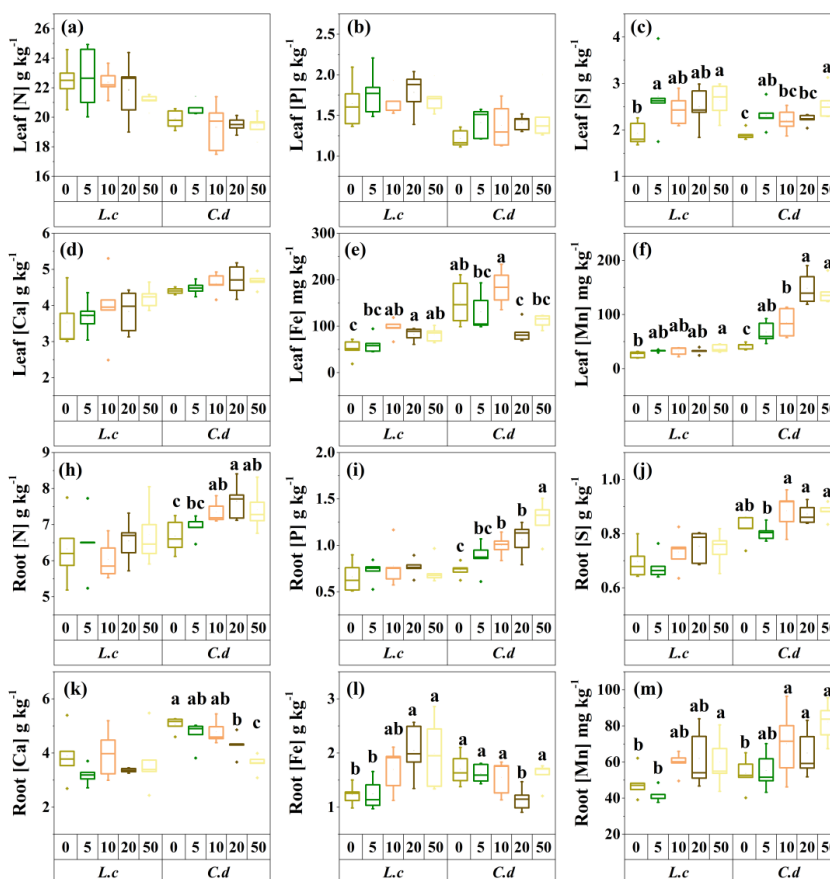


633

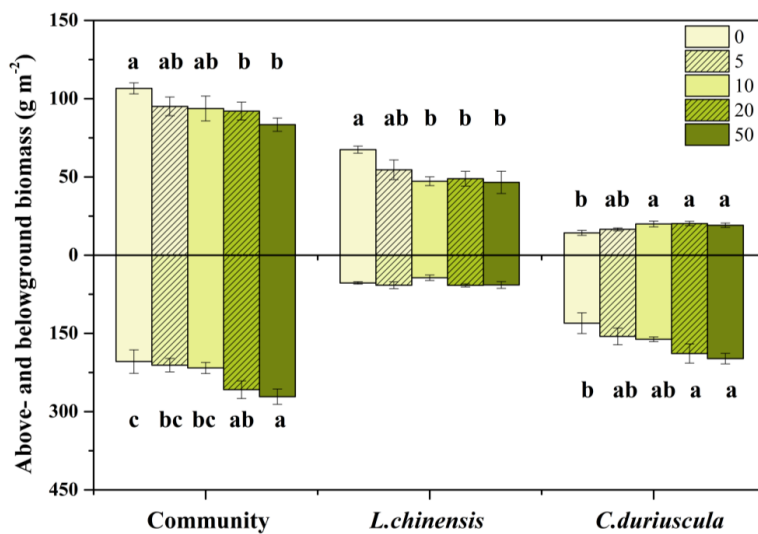
634 **Fig. 1** The response of the morphological traits to S addition for the two dominate  
 635 species in a meadow steppe. Abbreviations: SLA, Specific leaf area; LDMC, Leaf dry  
 636 matter content; SRL, specific root length; SRA, specific root area; RTD, root tissue  
 637 density; *L.c.*, *L. chinensis*; *C.d.*, *C. duriuscula*. Different letters above the bars indicate  
 638 significant influence among the S-addition level by one-way ANOVA at  $P < 0.05$ .

639





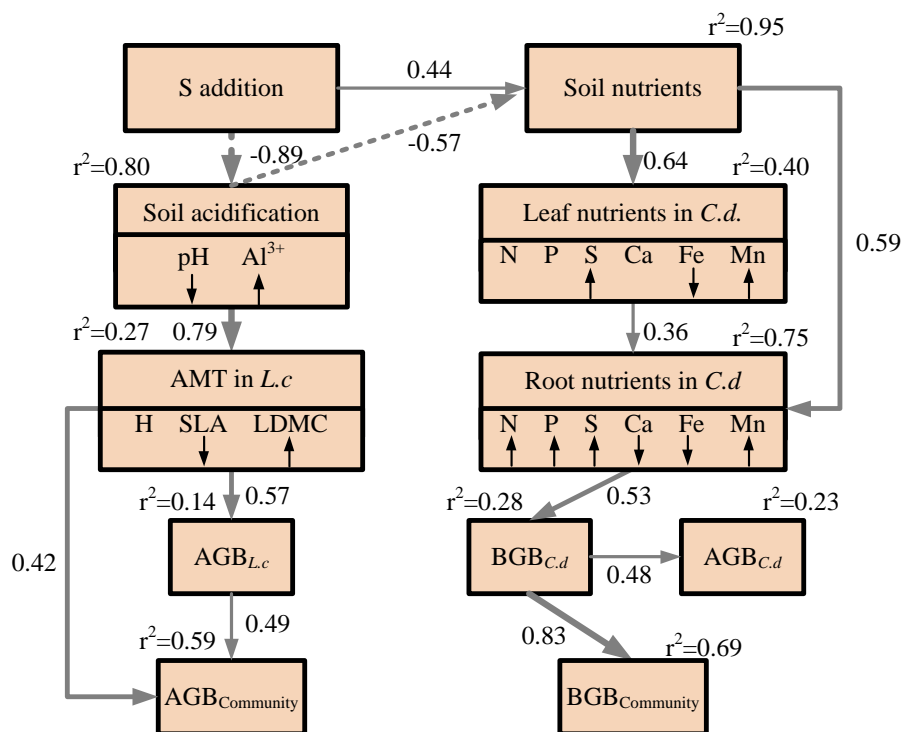
640  
 641 **Fig. 2** The response of the chemical traits to S addition for the two dominate species in  
 642 a meadow steppe. Abbreviations: Leaf [N], leaf N concentration; Leaf [P], leaf P  
 643 concentration; Leaf [S], leaf S concentration; Leaf [Ca], leaf Ca concentration; Leaf  
 644 [Fe], leaf Fe concentration; Leaf [Mn], leaf Mn concentration; Root [Ca], root Ca  
 645 concentration; Root [Fe], root Fe concentration; Root [Mn], root Mn concentration;  
 646 Root [N], root nitrogen concentration; Root [P], root phosphorus concentration; Root  
 647 [S], root sulfur concentration; *L.c.*, *L. chinensis*; *C.d.*, *C. duriuscula*. Different letters  
 648 above the bars indicate significant influence among the S-addition level by one-way  
 649 ANOVA at  $P < 0.05$ .  
 650



651  
 652 **Fig. 3** Effects of S addition on community and species aboveground and belowground  
 653 biomass. Bars are means  $\pm$  the standard error. Lower case letters indicate significant  
 654 difference among treatments ( $P < 0.05$ ).  
 655



656

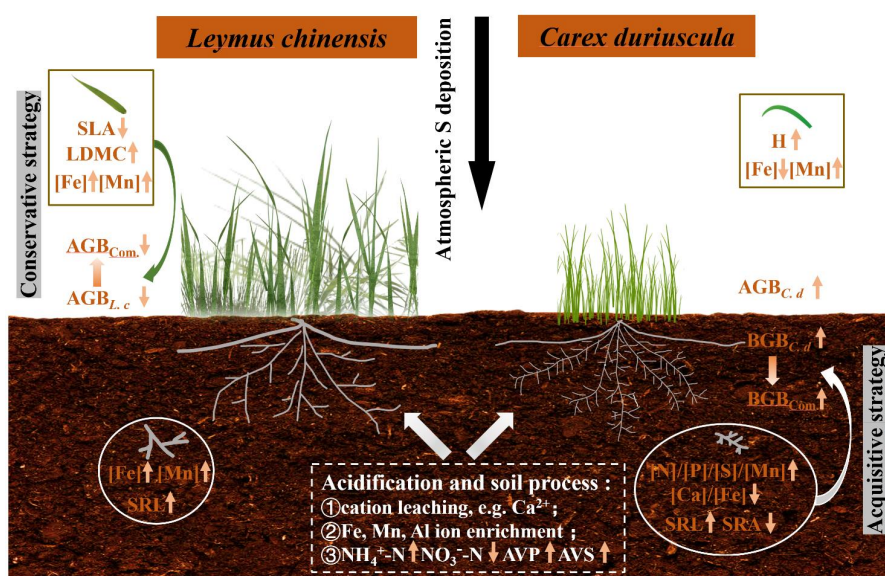


657

658 **Fig. 4** Structural equation model of S addition on plant community biomass through  
 659 the plausible pathways. Square boxes indicate the included variables in the analysis: S  
 660 addition; Soil nutrients include soil NH<sub>4</sub><sup>+</sup>-N and NO<sub>3</sub><sup>-</sup>-N concentrations, soil available  
 661 phosphorus, soil available sulfur; soil exchangeable cations Ca<sup>2+</sup>, Fe<sup>2+</sup> and Mn<sup>2+</sup>; soil  
 662 acidification includes soil pH and exchangeable Al<sup>3+</sup>; Aboveground morphological  
 663 traits (AMT) includes plant height, specific leaf area, leaf dry matter content in *L.*  
 664 *chinensis*; Leaf nutrients include leaf N, P, S, Ca, Fe, Mg concentrations in *C.*  
 665 *duriuscula*; Root nutrients include root N, P, S, Ca, Fe, Mg concentrations in *C.*  
 666 *duriuscula*; *C. duriuscula* aboveground biomass; *C. duriuscula* belowground biomass;  
 667 *L. chinensis* aboveground biomass; Community aboveground biomass and  
 668 belowground biomass. The symbols ↓ and ↑ indicate significant decrease or increase,  
 669 respectively, with increasing S addition. The final SEM adequately fitted the data:  $\chi^2 =$   
 670 51.83, DF = 40,  $P = 0.10$ , AIC = 103.83, n=25. R<sup>2</sup> values next to each response variable  
 671 indicate the proportion of variation explained by relationships with other variables.



672 Solid and dashed arrows represent significant positive and negative pathways ( $P < 0.05$ ),  
 673 respectively. Nonsignificant ( $P > 0.05$ ) pathways are not shown. Values at each arrow  
 674 indicate the standard path coefficient, which is equivalent to the correlation coefficient.  
 675  
 676



677  
 678 **Fig. 5** Schematic diagram illustrating the ecological effects of S-induced soil  
 679 acidification on above- and belowground biomass and traits of two dominant species in  
 680 a meadow steppe. ↑ = increase in response to S addition; ↓ = decrease in response to S  
 681 addition; Com. = Community; AVP = Soil available phosphorus; AVS = Soil available  
 682 sulfur.  
 683



684 **Table**

685 **Table 1** Effects of S addition on soil abiotic variables. All numbers refer to the mean  
 686 (the standard error). Lower case letters indicate significant difference among treatments  
 687 ( $P < 0.05$ ).

Soil parameters	S addition				
	0	5	10	20	50
Soil pH	6.95(0.06) a	6.70(0.07) ab	6.77(0.17) a	6.17(0.31) b	5.19 (0.20) c
Ex. Al <sup>3+</sup>	5.49(0.72) b	5.49(0.18) b	6.84(0.45) b	9.09(1.44) b	20.07(3.24) a
Ammonium	4.76(0.31) b	4.36(0.08) b	4.92(0.68) b	4.67(0.22) b	8.33(1.73) a
Nitrate	4.88(0.42) a	5.44(0.73) a	5.45(1.01) a	4.60(0.95) a	1.41(0.31) b
AVP	5.20(0.64) b	5.27(0.71) b	4.58(0.35) b	6.94(0.60) a	7.08(0.38) a
AVS	8.78(0.78) c	10.30(1.33) c	15.09(1.89) c	40.64(8.56) b	114.41(6.85) a
DTPA-Fe	22.10(1.14) c	27.94(0.02) bc	30.62(0.02) bc	38.07(0.04) b	58.72(0.07) a
DTPA-Mn	19.26(1.56) c	27.43(1.43) bc	33.23(3.10) bc	41.66(4.40) b	79.60(7.54) a
Ex. Ca <sup>2+</sup>	22.12(0.54) a	20.66(0.90) ab	20.14(1.09) ab	19.17(0.90) b	18.50(0.61) b

688 Note: Ex. Al<sup>3+</sup>: Exchangeable Al<sup>3+</sup>, mg kg<sup>-1</sup>; Ammonium: soil NH<sub>4</sub><sup>+</sup>-N concentration, mg kg<sup>-1</sup>;  
 689 Nitrate: soil NO<sub>3</sub><sup>-</sup>-N concentration, mg kg<sup>-1</sup>; AVP: soil available phosphorus, mg kg<sup>-1</sup>; AVS: soil  
 690 available sulfur, mg kg<sup>-1</sup>; DTPA-Fe: Soil DTPA-Fe concentration, mg kg<sup>-1</sup>; DTPA-Mn: Soil DTPA-  
 691 Mn concentration, mg kg<sup>-1</sup>; Ex. Ca: Exchangeable Ca<sup>2+</sup>, cmol kg<sup>-1</sup>.  
 692